# Advanced Numerical Methods for PDE Constrained Optimization with Application to Optimal Design in Navier Stokes Flow

Christian Brandenburg, Florian Lindemann, Michael Ulbrich and Stefan Ulbrich

**Abstract.** We present an approach to shape optimization which is based on transformation to a reference domain with continuous adjoint computations. This method is applied to the instationary Navier-Stokes equations for which we discuss the appropriate setting and discuss Fréchet differentiability of the velocity field with respect to domain transformations. Goal-oriented error estimation is used for an adaptive refinement strategy. Finally, we give some numerical results.

**Mathematics Subject Classification (2010).** Primary 76D55; Secondary 49K20.

**Keywords.** shape optimization, Navier-Stokes equations, PDE-constrained optimization, goal-oriented error estimation.

## 1. Introduction

This paper serves as the final report for the project "Advanced Numerical Methods for PDE Constrained Optimization with Application to Optimal Design and Control of a Racing Yacht in the America's Cup" in the DFG priority program 1253, *Optimization with Partial Differential Equations*. It covers some of the major results that were achieved in the course of the first funding period. The main task was to develop and investigate advanced numerical methods for finding the optimal shape of a body $B$, subject to constraints on the design, that is exposed to instationary incompressible Navier-Stokes flow. As an objective function the drag of the body was chosen in the numerical

We gratefully acknowledge the support of the Schwerpunktprogramm 1253 sponsored by the German Research Foundation (DFG). Part of the numerical computations were performed on a Linux cluster at TUM supported by DFG grant INST 95/919-1 FUGG. The work of the first and the fourth author was in parts supported by the International Research Training Group 1529 "Mathematical Fluid Dynamics" of the DFG.

computations. The resulting optimization problems are complex and highly nonlinear. As the developed techniques are quite general, they can, without significant conceptual difficulties, be used to address a wide class of shape optimization problems.

Shape optimization is an important and active field of research with many engineering applications; detailed accounts of its theory and applications can be found in, e.g., [8, 9, 15, 24, 28]. We use the approach of transformation to a reference domain, as originally introduced by Murat and Simon [26], see also [4, 14], which makes optimal control techniques readily applicable. Furthermore, as observed in [14] in the context of linear elliptic equations, and discussed in the present setting in [6], discretization and optimization can be made commutable. This allows to circumvent the tedious differentiation of finite element code with respect to the position of the vertices of the mesh.

We apply this approach to shape optimization problems governed by the instationary Navier-Stokes equations. On one hand we characterize the appropriate function spaces for domain transformations in this framework and give a theoretical result about the Fréchet differentiability of the design-to-state operator, which is done in section 2. On the other hand, we focus on the practical implementation of shape optimization methods. In section 3 we present the discretization and stabilization techniques we use to solve the Navier-Stokes equations numerically. Section 4 covers the use of goal-oriented error estimation and adaptivity for efficiently solving shape optimization problems. We then present numerical results obtained for some model problems in section 5, followed by some conclusions in section 6.

## 2. Shape optimization for the Navier-Stokes equations

### 2.1. Shape Optimization in the abstract setting

We use the approach of transformation to a reference domain to formulate the optimization problem in a functional analytical setting. The idea of using transformations to describe varying domains was suggested by Murat and Simon, see [26], and forms an excellent basis for deriving rigorous Fréchet differentiability results with respect to domain variations [4, 14]. This approach provides a flexible framework that can be used for many types of transformations (e.g., boundary displacements, free form deformation).

We consider a reference domain $\Omega_{\mathrm{ref}}$ and interpret admissible domains $\Omega \in \mathcal{O}_{\mathrm{ad}}$ as images of $\Omega_{\mathrm{ref}}$ under suitable transformations $\tau$. Then the abstract optimization problem is given as:

$$\min \quad J(y,\tau) \quad \text{s.t.} \quad E(y,\tau) = 0, \quad \tau \in T_{\mathrm{ad}}. \tag{2.1}$$

We minimize an objective functional $J : Y(\Omega_{\mathrm{ref}}) \times T(\Omega_{\mathrm{ref}}) \to \mathbb{R}$ where the state $y \in Y(\Omega_{\mathrm{ref}})$ and the transformation $\tau \in T(\Omega_{\mathrm{ref}})$ are coupled by the *state equation* $E(y,\tau) = 0$ with $E : Y(\Omega_{\mathrm{ref}}) \times T(\Omega_{\mathrm{ref}}) \to Z(\Omega_{\mathrm{ref}})$. Here, $T_{\mathrm{ad}} \subset T(\Omega_{\mathrm{ref}})$ is the set of admissible transformations corresponding to the set of admissible domains $\mathcal{O}_{\mathrm{ad}}$. $T(\Omega_{\mathrm{ref}}) \subset \{\tau : \Omega_{\mathrm{ref}} \to \mathbb{R}^d\}$, $d = 2$ or 3, is

assumed to be a Banach space of bicontinuous transformations of $\Omega_{\rm ref}$. In this context, $Y(\Omega)$ is a Banach space of functions defined on $\Omega \subset \mathbb{R}^d$ and we assume that

$$\left.\begin{array}{c} Y(\Omega_{\rm ref}) = \{\tilde{y} \circ \tau : \tilde{y} \in Y(\tau(\Omega_{\rm ref}))\} \\ \tilde{y} \in Y(\tau(\Omega_{\rm ref})) \mapsto y := \tilde{y} \circ \tau \in Y(\Omega_{\rm ref}) \text{ is a homeomorphism} \end{array}\right\} \quad \forall\, \tau \in T_{\rm ad}. \tag{A}$$

If the state equation is given in variational form defined on the domain $\tau(\Omega_{\rm ref})$, then usually an equivalent variational form $E$ defined on the reference domain can be obtained by using the transformation rule for integrals. This will be demonstrated for the instationary Navier-Stokes equations in the following. By convention, we denote all quantities on the physical domains $\tau(\Omega_{\rm ref})$ by $\tilde{}$.

### 2.2. The Navier-Stokes equations

We apply the presented approach to shape optimization problems governed by the instationary Navier-Stokes equations for a viscous, incompressible fluid on a bounded domain $\Omega = \tau(\Omega_{\rm ref}) \subset \mathbb{R}^d$ with Lipschitz boundary. To avoid technicalities in the formulation of the equations, we consider homogeneous Dirichlet boundary conditions. We arrive at the problem

$$\begin{aligned} \tilde{\boldsymbol{v}}_t - \nu\Delta\tilde{\boldsymbol{v}} + (\tilde{\boldsymbol{v}}\cdot\nabla)\tilde{\boldsymbol{v}} + \nabla\tilde{p} = \tilde{\boldsymbol{f}} \quad &\text{on } \Omega\times I, \;\; \operatorname{div}\tilde{\boldsymbol{v}} = 0 \quad \text{on } \Omega\times I \\ \tilde{\boldsymbol{v}} = \boldsymbol{0} \quad &\text{on } \partial\Omega\times I, \;\; \tilde{\boldsymbol{v}}(\cdot,0) = \tilde{\boldsymbol{v}}_0 \quad \text{on } \Omega \end{aligned}$$

where $\tilde{\boldsymbol{v}} : \Omega \times I \to \mathbb{R}^d$ denotes the velocity and $\tilde{p} : \Omega \times I \to \mathbb{R}$ the pressure of the fluid. Here $I = (0,T), T > 0$ is the time interval and $\nu > 0$ is the kinematic viscosity.

We introduce the spaces

$$\mathcal{V}(\Omega) := \{\tilde{\boldsymbol{v}} \in C_0^\infty(\Omega)^d : \; \operatorname{div}\tilde{\boldsymbol{v}} = 0\}, \quad V(\Omega) := \operatorname{cl}_{H_0^1}(\mathcal{V}(\Omega)),$$

$$H(\Omega) := \operatorname{cl}_{L^2}(\mathcal{V}(\Omega)), \quad L_0^2(\Omega) := \{\tilde{p} \in L^2(\Omega) : \int_\Omega \tilde{p} = 0\},$$

the corresponding Gelfand triple $V(\Omega) \hookrightarrow H(\Omega) \hookrightarrow V(\Omega)^*$, and define

$$W(I;V(\Omega)) := \{\tilde{\boldsymbol{v}} \in L^2(I;V(\Omega)) : \; \tilde{\boldsymbol{v}}_t \in L^2(I;V(\Omega)^*)\}.$$

In the same way, the space $W(I;H_0^1(\Omega)^d)$ used later is defined.

Now let $\tilde{\boldsymbol{f}} \in L^2(I;H^{-1}(\Omega)^d), \tilde{\boldsymbol{v}}_0 \in H(\Omega)$. It is well known that so far the question of existence and uniqueness is answered satisfactorily only in the case $d \le 2$. In fact, under these assumptions with $d = 2$, there exists a unique solution $(\tilde{\boldsymbol{v}}, \tilde{p})$ with $\tilde{\boldsymbol{v}} \in W(I;V(\Omega))$ where $\tilde{p}$ is a $L_0^2(\Omega)$-valued distribution, see [30]. Assuming that the data $\tilde{\boldsymbol{f}}$ and $\tilde{\boldsymbol{v}}_0$ are sufficiently regular, the solution has further regularity as stated by

**Lemma 2.1.** *Let $d = 2$ and assume*

$$\tilde{\boldsymbol{f}}, \tilde{\boldsymbol{f}}_t \in L^2(I;H^{-1}(\Omega)^2), \tilde{\boldsymbol{f}}(\cdot,0) \in H, \tilde{\boldsymbol{v}}_0 \in V(\Omega) \cap H^2(\Omega)^2. \tag{2.2}$$

*Then the solution $(\tilde{\boldsymbol{v}}, \tilde{p})$ of the Navier-Stokes equations satisfies*

$$\tilde{\boldsymbol{v}} \in C(I;V(\Omega)), \;\; \tilde{\boldsymbol{v}}_t \in L^2(I,V(\Omega)) \cap L^\infty(I;H(\Omega)), \;\; \tilde{p} \in L^\infty(I;L_0^2(\Omega)) \tag{2.3}$$

The proof can be found for example in [30, Ch. III].

### 2.3. Weak formulation and transformation to the reference domain

Under the assumptions of Lemma 2.1, we consider a weak velocity-pressure formulation of the problem where the divergence-freeness of the velocity is not+included in the trial and test spaces: Find $(\tilde{\boldsymbol{v}}, \tilde{p})$ such that

$$\begin{aligned}
&\langle \tilde{\boldsymbol{v}}_t(\cdot,t), \tilde{\boldsymbol{w}} \rangle_{H^{-1},H_0^1} + \int_\Omega \tilde{\boldsymbol{v}}(x,t)^T \nabla \tilde{\boldsymbol{v}}(x,t) \tilde{\boldsymbol{w}}(x)\,dx + \int_\Omega \nu \nabla \tilde{\boldsymbol{v}}(x,t) : \nabla \tilde{\boldsymbol{w}}(x)\,dx \\
&- \int_\Omega \tilde{p}(x,t)\ \operatorname{div} \tilde{\boldsymbol{w}}(x)\,dx = \int_\Omega \tilde{\boldsymbol{f}}(x,t)^T \tilde{\boldsymbol{w}}(x)\,dx \quad \forall\, \tilde{\boldsymbol{w}} \in H_0^1(\Omega)^d \text{ for a.a. } t \in I \\
&\int_\Omega \tilde{q}(x)\ \operatorname{div} \tilde{\boldsymbol{v}}(x,t)\,dx = 0 \qquad\qquad \forall\, \tilde{q} \in L_0^2(\Omega) \text{ for a.a. } t \in I \\
&\tilde{\boldsymbol{v}}(\cdot,0) = \tilde{\boldsymbol{v}}_0.
\end{aligned} \tag{2.4}$$

In the following we assume that

(T) $\Omega_{\text{ref}}$ is a bounded Lipschitz domain and $\Omega' \supset \bar{\Omega}_{\text{ref}}$ is open and bounded with Lipschitz boundary. Moreover $T_{\text{ad}} \subset W^{2,\infty}(\Omega')^d$ is bounded such that for all $\tau \in T_{\text{ad}}$ the mappings $\tau : \bar{\Omega}_{\text{ref}} \to \tau(\bar{\Omega}_{\text{ref}})$ satisfy $\tau^{-1} \in W^{2,\infty}(\tau(\bar{\Omega}_{\text{ref}}))^d$ and $\det(\tau') \geq \delta > 0$, with a constant $\delta > 0$. Here, $\tau'(x) = \nabla \tau(x)^T$ denotes the Jacobian of $\tau$.
Moreover, the data $\tilde{\boldsymbol{v}}_0, \tilde{\boldsymbol{f}}$ are given such that

$$\begin{aligned}
&\tilde{\boldsymbol{f}} \in L^\infty(I; C^1(\Omega)^d),\ \tilde{\boldsymbol{f}}_t \in L^2(I; H^{-1}(\Omega)^d), \\
&\tilde{\boldsymbol{f}}(0) \in H(\Omega),\ \tilde{\boldsymbol{v}}_0 \in V(\Omega) \cap H^2(\Omega)^d \cap C^1(\Omega)^d
\end{aligned}$$

for all $\Omega \in \mathcal{O}_{\text{ad}} = \{\tau(\Omega_{\text{ref}}) \ :\ \tau \in T_{ad}\}$, i.e., the data $\tilde{\boldsymbol{v}}_0, \tilde{\boldsymbol{f}}_0$ are used on all $\Omega \in \mathcal{O}_{\text{ad}}$.

Assumption (T) ensures in particular (2.2) and assumption (A) holds in the following obvious version for time dependent problems, where the transformation acts only in space.

**Lemma 2.2.** *Let $T_{ad}$ satisfy assumption* (T)*. Then the space $W(I; H_0^1(\Omega)^d)$ for the velocity satisfies assumption* (A)*, more precisely, we have for all $\tau \in T_{ad}$*

$$\begin{aligned}
&W(I; H_0^1(\Omega_{\text{ref}})^d) = \{\tilde{\boldsymbol{v}}(\tau(\cdot)) : \tilde{\boldsymbol{v}} \in W(I; H_0^1(\tau(\Omega_{\text{ref}}))^d)\}, \\
&\tilde{\boldsymbol{v}} \in W(I; H_0^1(\tau(\Omega_{\text{ref}}))^d) \mapsto \boldsymbol{v} := \tilde{\boldsymbol{v}}(\tau(\cdot)) \in W(I; H_0^1(\Omega_{\text{ref}})^d) \text{ is a homeom.}
\end{aligned}$$

A proof of this result is beyond the scope of this paper and will be given in [20]. A similar result can be shown for the pressure if we define a topology on the pressure space like $L^p(I; L_0^2(\Omega))$ as guaranteed by lemma 2.1.

Given the weak formulation of the Navier-Stokes equations on a domain $\tau(\Omega_{\text{ref}})$ we can apply the transformation rule for integrals to obtain a variational formulation based on the domain $\Omega_{\text{ref}}$ which is equivalent to (2.4):

Find $(\boldsymbol{v}, p) \in W(I; H_0^1(\Omega_{\text{ref}})^d) \times \{p \mid p(\cdot, t) \in L_0^2(\Omega_{\text{ref}}) \ \forall t \in I\}$ such that

$$\begin{aligned}
&\int_{\Omega_{\text{ref}}} \boldsymbol{v}_t^T \boldsymbol{w} \det \tau' \, dx + \sum_{i=1}^{d} \int_{\Omega_{\text{ref}}} \nu \nabla v_i^T \tau'^{-1} \tau'^{-T} \nabla w_i \det \tau' \, dx \\
&+ \int_{\Omega_{\text{ref}}} \boldsymbol{v}^T \tau'^{-T} \nabla \boldsymbol{v} \ \boldsymbol{w} \det \tau' \ dx - \int_{\Omega_{\text{ref}}} p \ \operatorname{tr}(\tau'^{-T} \nabla \boldsymbol{w}) \det \tau' \, dx \\
&- \int_{\Omega_{\text{ref}}} \tilde{\boldsymbol{f}}(\tau(x), t)^T \boldsymbol{w} \det \tau' \, dx = 0 \quad \forall \boldsymbol{w} \in H_0^1(\Omega_{\text{ref}})^d \text{ for a.a. } t \in I \\
&\int_{\Omega_{\text{ref}}} q \ \operatorname{tr}(\tau'^{-T} \nabla \boldsymbol{v}) \det \tau' \, dx = 0 \quad \forall q \in L_0^2(\Omega_{\text{ref}}) \text{ for a.a. } t \in I \\
&\boldsymbol{v}(\cdot, 0) = \tilde{\boldsymbol{v}}_0(\tau(\cdot)).
\end{aligned} \tag{2.5}$$

### 2.4. Differentiability of the design-to-state operator

Very recently, we succeeded in proving Fréchet differentiability of the velocity field with respect to domain variations in 2D under reasonable assumptions. In the following, we consider the case $d = 2$. A paper on these results is in preparation [20]. For the stationary Navier-Stokes equations, a corresponding investigation can be found in [4]. Significant additional complications for the time-dependent case are caused by the fact that in the standard $W(I; V(\Omega))$-setting the time regularity of the pressure is very low. In fact, the $\nabla \tilde{p}$ term takes care of those parts of the residual that are not seen when tested with solenoidal functions. Now $L^2(I; V(\Omega)^*)$ is a weaker space than $L^2(I; H^{-1}(\Omega)^2)$, since $V(\Omega) \subsetneq H_0^1(\Omega)^2$ is a closed subspace strictly smaller than $H_0^1(\Omega)^2$. Therefore, the fact that $\tilde{\boldsymbol{v}}_t \in L^2(I; V(\Omega)^*)$ cannot be used to derive time regularity results for the pressure. This causes difficulties since after transformation to the reference domain the velocity field is no longer solenoidal. Thus, the pressure cannot be eliminated and the skew symmetry of the trilinear convection form cannot be used since it only holds if the first argument is solenoidal. For achieving that the required regularity properties of solutions are maintained under transformation, we need the requirement $\tau \in T_{\text{ad}} \subset W^{2,\infty}(\Omega')^2$. This especially concerns the regularity of the time derivative. As already discussed, in 2D, the Navier-Stokes equations on the domain $\Omega = \tau(\Omega_{\text{ref}})$ have a unique solution $\tilde{\boldsymbol{v}} \in W(I; V(\Omega))$. Under the assumptions stated in Lemma 2.1, there also holds

$$\tilde{\boldsymbol{v}} \in C(I; V(\Omega)), \quad \tilde{\boldsymbol{v}}_t \in L^2(I; V(\Omega)) \cap L^\infty(I; H(\Omega)). \tag{2.6}$$

This implies the pressure regularity $\tilde{p} \in L^\infty(I; L_0^2(\Omega))$. The latter regularity properties are maintained under transformation to the reference domain $\Omega_{\text{ref}}$. After transformation of the Navier-Stokes equations, the condition $\operatorname{div} \tilde{\boldsymbol{v}} = 0$ becomes $\operatorname{tr}(g(\tau')\nabla \boldsymbol{v}) = 0$, where $g(M) = \det M \, M^{-T}$. To proceed further, it is crucial to require and exploit the additional regularity of $\boldsymbol{v}$. As demonstrated in [4, 6], it is sufficient to consider the differentiability of $\boldsymbol{v}(\tau)$ at $\tau = \text{id}$, since $\tau(\Omega_{\text{ref}})$ can be taken as the current reference

domain and the derivative w.r.t. variations of this domain can be transformed to derivatives w.r.t. domain variations of $\Omega_{\text{ref}}$. We build on the uniform boundedness of $\boldsymbol{v}(\tau)$ in the sense of (2.6) for $\tau$ sufficiently close to id. In a first step, we prove continuity results for the solution operator $\tau \mapsto \boldsymbol{v}(\tau)$ in $L^\infty(I; L^2(\Omega)^2) \cap L^2(I; H_0^1(\Omega)^2)$. From this and the boundedness in (2.6), continuity in stronger spaces can be proved, e.g., by interpolation.

For further presentation, we write the equations (2.5) on $\Omega_{\text{ref}}$ schematically as

$$E(\boldsymbol{v}, p, \tau) = 0.$$

Formal linearization of (2.5) about $(\bar{\boldsymbol{v}}, \bar{p}, \bar{\tau}) = (\boldsymbol{v}(\mathrm{id}), p(\mathrm{id}), \mathrm{id})$ yields

$$A_1(\bar{\boldsymbol{v}}, \mathrm{id})\delta\boldsymbol{v} + A_2(\mathrm{id})\delta p + A_3(\bar{\boldsymbol{v}}, \bar{p}, \mathrm{id})\delta\tau = 0.$$

As mentioned, $\delta\boldsymbol{v}$ is not solenoidal, but satisfies $\operatorname{div}(\delta\boldsymbol{v}) = -\operatorname{tr}(g'(I)\delta\tau'\nabla\bar{\boldsymbol{v}})$ with $g(M)$ as defined above. To apply standard theory, we use the existence of a right inverse $B : L_0^2(\Omega_{\text{ref}}) \to H_0^1(\Omega_{\text{ref}})^2$ of the div operator that, as shown in [13], can be chosen such that it also is a bounded linear operator from $H^1(\Omega_{\text{ref}})^*$ to $L_0^2(\Omega_{\text{ref}})^2$. We set $\boldsymbol{e}_0 = -B\operatorname{tr}(g'(I)\delta\tau'\nabla\bar{\boldsymbol{v}})$ and obtain a splitting $\delta\boldsymbol{v} = \boldsymbol{e}_0 + \boldsymbol{e}$, where now $\boldsymbol{e}$ is solenoidal. Note that $\boldsymbol{e}_0 = A_4(\nabla\bar{\boldsymbol{v}}, \delta\tau')$ is bilinear. Inserting $\delta\boldsymbol{v} = \boldsymbol{e}_0 + \boldsymbol{e}$ into the linearized equation gives a linearized Navier-Stokes equation for the solenoidal function $\boldsymbol{e}$. The right hand side generated by $\boldsymbol{e}_0$ can be carefully estimated to obtain linear bounds for $\delta\boldsymbol{v}$ in terms of $\delta\tau$. Clearly, $\delta\boldsymbol{v}$ is the candidate for the derivative $\boldsymbol{v}_\tau(\mathrm{id})\delta\tau$, if it exists. Next, we consider, with $\tau = \mathrm{id} + \delta\tau$, $\boldsymbol{v} = \boldsymbol{v}(\tau)$, and $p = p(\tau)$ the equation

$$E(\boldsymbol{v}, p, \tau) - E(\bar{\boldsymbol{v}}, \bar{p}, \mathrm{id}) - [A_1(\bar{\boldsymbol{v}}, \mathrm{id})\delta\boldsymbol{v} + A_2(\mathrm{id})\delta p + A_3(\bar{\boldsymbol{v}}, \bar{p}, \mathrm{id})\delta\tau] = 0.$$

This is rearranged to obtain a linear equation for the residual $(\boldsymbol{r}, r_p) = (\boldsymbol{v} - \bar{\boldsymbol{v}} - \delta\boldsymbol{v}, p - \bar{p} - \delta p)$ while the remaining terms are taken to the right hand side. Again $\boldsymbol{r}$ is not solenoidal and using the operator $B$ the splitting $\boldsymbol{r} = \boldsymbol{r}_0 + \boldsymbol{r}_1$ is obtained such that $\boldsymbol{r}_1$ is solenoidal. Now, again, standard theory for the linearized Navier-Stokes equations can be used, where the estimation of the right hand side is quite involved. Taking all together, the following can be shown.

**Theorem 2.3.** *Let the assumption (T) hold. Then the operator*

$$\tau \in T_{ad} \subset W^{2,\infty}(\Omega')^2 \mapsto \boldsymbol{v}(\tau) \in W(I; H_0^1(\Omega_{ref})^2) + W(I; V(\Omega_{ref}))$$

*is Fréchet differentiable. Note that the range space is continuously imbedded into* $L^2(I; H_0^1(\Omega_{ref})^2) \cap C(I; L^2(\Omega_{ref})^2)$.

This result implies for example that the time averaged drag on a body $B$ depends differentiable on $\tau$, since it can be rewritten in an appropriate distributed form, see [6].

### 2.5. Shape gradient calculation with the Navier-Stokes equations

As for every $\tau \in T_{\mathrm{ad}}$ there exists a unique solution $(\boldsymbol{v}, p)$ of the Navier-Stokes equations, it is reasonable to define the following reduced problem on the space of transformations $T(\Omega_{\mathrm{ref}})$:

$$\min j(\tau) := J(y(\tau), \tau) \qquad \text{s.t.} \quad \tau \in T_{\mathrm{ad}},$$

where $y(\tau)$ is given as the solution of the transformed Navier-Stokes equations (2.5).

In order to calculate the gradient of $j$ we need to solve the adjoint equations of the transformed Navier-Stokes equations (2.5).
Given a weak solution $(\boldsymbol{v}, p) \in Y(\Omega_{\mathrm{ref}}) := W(I; H_0^1(\Omega_{\mathrm{ref}})^d) \times L^2(I; L_0^2(\Omega_{\mathrm{ref}}))$ we seek $(\boldsymbol{\lambda}, \mu) \in L^2(I; H_0^1(\Omega_{\mathrm{ref}})^d) \times L^2(I; L_0^2(\Omega_{\mathrm{ref}}))$ with

$$\begin{aligned}
&- \int_I \int_{\Omega_{\mathrm{ref}}} \boldsymbol{w}^T \boldsymbol{\lambda}_t \det \tau' \; dt \; dx + \int_{\Omega_{\mathrm{ref}}} \boldsymbol{w}(x,T)^T \boldsymbol{\lambda}(x,T) \det \tau' \; dx \\
&+ \int_I \sum_{i=1}^{d} \int_{\Omega_{\mathrm{ref}}} \nu \nabla w_i^T \tau'^{-1} \tau'^{-T} \nabla \lambda_i \det \tau' \; dx \; dt \\
&+ \int_I \int_{\Omega_{\mathrm{ref}}} \left( \boldsymbol{w}^T \tau'^{-T} \nabla \boldsymbol{v} + \boldsymbol{v}^T \tau'^{-T} \nabla \boldsymbol{w} \right) \boldsymbol{\lambda} \det \tau' \; dx \; dt \\
&- \int_I \int_{\Omega_{\mathrm{ref}}} q \; \mathrm{tr}(\tau'^{-T} \nabla \boldsymbol{\lambda}) \det \tau' \; dx \; dt + \int_I \int_{\Omega_{\mathrm{ref}}} \mu \; \mathrm{tr}(\tau'^{-T} \nabla \boldsymbol{w}) \det \tau' \; dx \; dt \\
&= -\langle J_{(\boldsymbol{v},p)}((\boldsymbol{v},p),\tau), (\boldsymbol{w},q) \rangle_{Y^*(\Omega_{\mathrm{ref}}), Y(\Omega_{\mathrm{ref}})} \quad \forall (\boldsymbol{w},q) \in Y(\Omega_{\mathrm{ref}}).
\end{aligned}$$

This is a parabolic equation backwards in time with appropriate initial condition for the adjoint velocity $\boldsymbol{\lambda}$ at time $T$ depending on the objective functional. For details, we refer to [6]. For $\tau = \mathrm{id}$, we arrive at the weak formulation of the usual adjoint system of the Navier-Stokes equations on $\Omega_{\mathrm{ref}}$.

For the application of optimization algorithms it is convenient to solve, for a given iterate $\tau_k \in T(\Omega_{\mathrm{ref}})$, an equivalent representation of the optimization problem on the domain $\Omega_k := \tau_k(\Omega_{\mathrm{ref}})$ (for details see [6]). Without loss of generality we assume $\Omega_k = \Omega_{\mathrm{ref}}$ and calculate the reduced gradient $j'(\tau)$ at $\tau = \mathrm{id}$:

1. Find $(\boldsymbol{v}, p)$ by solving the standard Navier-Stokes equations on the domain $\Omega_{\mathrm{ref}}$.
2. Find $(\boldsymbol{\lambda}, \mu)$ by solving the standard adjoint Navier-Stokes equations on the domain $\Omega_{\mathrm{ref}}$.

3. Calculate the reduced gradient $j'(\mathrm{id})$ via

$$
\begin{aligned}
&\langle j'(\mathrm{id}), V\rangle_{T^*(\Omega_{\mathrm{ref}}),T(\Omega_{\mathrm{ref}})} = \langle J_\tau((\boldsymbol{v},p),\tau), V\rangle_{T^*(\Omega_{\mathrm{ref}}),T(\Omega_{\mathrm{ref}})} \\
&- \int_{\Omega_{\mathrm{ref}}} V^T \nabla \tilde{\boldsymbol{v}}_0(x)\boldsymbol{\lambda}(x,0)\; dx + \int_I \int_{\Omega_{\mathrm{ref}}} \boldsymbol{v}_t^T \boldsymbol{\lambda} \operatorname{div} V \; dx \; dt \\
&+ \int_I \int_{\Omega_{\mathrm{ref}}} \nu \nabla \boldsymbol{v} : \nabla \boldsymbol{\lambda} \operatorname{div} V \; dx \; dt - \sum_{i=1}^{d} \int_I \int_{\Omega_{\mathrm{ref}}} \nu \nabla \boldsymbol{v}_i^T (V' + V'^T) \nabla \boldsymbol{\lambda}_i \; dx \; dt \\
&- \int_I \int_{\Omega_{\mathrm{ref}}} \boldsymbol{v}^T V'^T \nabla \boldsymbol{v} \boldsymbol{\lambda} \; dx \; dt + \int_I \int_{\Omega_{\mathrm{ref}}} \boldsymbol{v}^T \nabla \boldsymbol{v} \boldsymbol{\lambda} \operatorname{div} V \; dx \; dt \\
&+ \int_I \int_{\Omega_{\mathrm{ref}}} p \operatorname{tr}(V'^T \nabla \boldsymbol{\lambda}) \; dx \; dt - \int_I \int_{\Omega_{\mathrm{ref}}} p \operatorname{div} \boldsymbol{\lambda} \operatorname{div} V \; dx \; dt \\
&- \int_I \int_{\Omega_{\mathrm{ref}}} \tilde{\boldsymbol{f}}^T \boldsymbol{\lambda} \operatorname{div} V \; dx \; dt - \int_I \int_{\Omega_{\mathrm{ref}}} V^T \nabla \tilde{\boldsymbol{f}} \boldsymbol{\lambda} \; dx \; dt \\
&- \int_I \int_{\Omega_{\mathrm{ref}}} \mu \operatorname{tr}(V'^T \nabla \boldsymbol{v}) \; dx \; dt + \int_I \int_{\Omega_{\mathrm{ref}}} \mu \operatorname{div} \boldsymbol{v} \operatorname{div} V \; dx \; dt.
\end{aligned}
\tag{2.7}
$$

Finally, if we assume more regularity for the state and adjoint, we can integrate by parts in the above formula and can represent the shape gradient as a functional on the boundary. However, we prefer to work with the distributed version (2.7), since it is also appropriate for FE-Galerkin approximations, while the integration by parts to obtain the boundary representation is not justified for FE-discretizations with $H^1$-elements.

### 2.6. Derivatives with respect to shape parameters

In practical situations, the domain transformations $\tau$ are usually not given directly. Instead, one often deals with design parameters $u \in U$ where $U$ is a finite or infinite dimensional design space defining the boundary $\Gamma_B$ of the design object. Possible choices for the design parameters $u$ are e.g. B-spline control points or even the boundary curve itself. In this context, the reduced gradient of the objective function w.r.t $u$ can be computed in a very efficient way.

First of all, $u$ defines a displacement $d(u)$ of the reference object boundary $\Gamma_B$. Sensitivities for this mapping are usually easy to calculate, e.g. for B-Spline parametrizations $d(u)$ is a linear function w.r.t. the B-Spline control points $u$. The boundary displacement $d(u)$ can then be mapped to a domain transformation $\tau(u)$ by solving for example an elliptic PDE (e.g., linear elasticity equation or Poisson equation) with fixed displacement $d(u)$ on the object boundary and homogeneous Dirichlet boundary conditions on $\partial\Omega_{\mathrm{ref}} \setminus \Gamma_B$. In the case of the elasticity equation this leads to an optimization problem of the form

$$
\min \quad j(\tau) \quad \text{s.t.} \quad A\,(\tau, d(u)) = 0, \quad u \in U_{\mathrm{ad}}, \tag{2.8}
$$

where $A$ denotes the elasticity equation with boundary conditions. Using adjoint calculus, we get

$$
\tilde{j}_d(d(u)) = A_d(\tau, d(u))^* z,
$$

where $\tilde{j} := j(\tau(d(u))$ denotes the reduced objective functional w.r.t $d(u)$ and $z$ is the solution of the adjoint elasticity equation

$$\langle A_\tau(\tau, d(u))V, z\rangle_{T^*(\Omega_{\rm ref}),T(\Omega_{\rm ref})} = -\langle j'(\tau), V\rangle_{T^*(\Omega_{\rm ref}),T(\Omega_{\rm ref})} \qquad \forall V \in T(\Omega_{\rm ref}).$$

Note that the right hand side is just (2.7) and that the evaluation of this equation makes up the main part of the work for computing the reduced derivative. Derivatives of $\tilde{j}$ w.r.t. $u$ are then easily obtained by the chain rule and are given by

$$\frac{d}{du}\tilde{j}(d(u)) = d_u(u)^* A_d(\tau, d(u))^* z.$$

## 3. Discretization

To discretize the instationary Navier-Stokes equations, we use the $cG(1)dG(0)$ space-time finite element method, which uses piecewise constant finite elements in time and piecewise linear finite elements in space and is a variant of the General Galerkin $G^2$-method developed by Eriksson et al. [11, 12].

Let $\mathcal{I} = \{I_j = (t_{j-1}, t_j] : 1 \le j \le N\}$ be a partition of the time interval $(0, T]$ with a sequence of discrete time steps $0 = t_0 < t_1 < \cdots < t_N = T$ and length of the respective time intervals $k_j := |I_j| = t_j - t_{j-1}$. With each time step $t_j$, we associate a partition $\mathcal{T}_j$ of the spatial domain $\Omega$ and the finite element subspaces $V_h^j, P_h^j$ of continuous piecewise linear functions in space.

The $cG(1)dG(0)$ space-time finite element discretization with stabilization can be written as an implicit Euler scheme: $\tilde{\boldsymbol{v}}_h^0 = \tilde{\boldsymbol{v}}_0$ and for $j = 1 \dots N$, find $(\tilde{\boldsymbol{v}}_h^j, \tilde{p}_h^j) \in V_h^j \times P_h^j$ such that

$$\left(\bar{E}^{h,j}(\tilde{\boldsymbol{v}}_h, \tilde{p}_h), (\tilde{\boldsymbol{w}}_h, \tilde{q}_h)\right) + \left(\bar{SD}_\delta^j(\tilde{\boldsymbol{v}}_h, \tilde{p}_h), (\tilde{\boldsymbol{w}}_h, \tilde{q}_h)\right) = 0 \qquad \forall (\tilde{\boldsymbol{w}}_h, \tilde{q}_h)_{|_{I_j}} \in V_h^j \times P_h^j$$

with the discretized Navier-Stokes equations

$$\left(\bar{E}^{h,j}(\tilde{\boldsymbol{v}}_h, \tilde{p}_h), (\tilde{\boldsymbol{w}}_h, \tilde{q}_h)\right) := \left(\frac{\tilde{\boldsymbol{v}}_h^j - \tilde{\boldsymbol{v}}_h^{j-1}}{k_j}, \tilde{\boldsymbol{w}}_h^j\right) + (\nu\nabla\tilde{\boldsymbol{v}}_h^j, \nabla\tilde{\boldsymbol{w}}_h^j) + (\tilde{\boldsymbol{v}}_h^j \cdot \nabla\tilde{\boldsymbol{v}}_h^j, \tilde{\boldsymbol{w}}_h^j) - (\tilde{p}_h^j,\ \mathrm{div}\ \tilde{\boldsymbol{w}}_h^j) + (\ \mathrm{div}\ \tilde{\boldsymbol{v}}_h^j, \tilde{q}_h^j) - (\tilde{\boldsymbol{f}}, \tilde{\boldsymbol{w}}_h^j)\ ,$$

and with the stabilization

$$\left(\bar{SD}_\delta^j(\tilde{\boldsymbol{v}}_h, \tilde{p}_h), (\tilde{\boldsymbol{w}}_h, \tilde{q}_h)\right) := \left(\tilde{\delta}_1(\tilde{\boldsymbol{v}}_h^j \cdot \nabla\tilde{\boldsymbol{v}}_h^j + \nabla\tilde{p}_h^j - \tilde{\boldsymbol{f}}), \tilde{\boldsymbol{v}}_h^j \cdot \nabla\tilde{\boldsymbol{w}}_h^j + \nabla\tilde{q}_h^j\right) + (\tilde{\delta}_2\ \mathrm{div}\ \tilde{\boldsymbol{v}}_h^j,\ \mathrm{div}\ \tilde{\boldsymbol{w}}_h^j)\ .$$

Note that the terms $(\tilde{\boldsymbol{v}}_h^j)_t - \nu\Delta\tilde{\boldsymbol{v}}_h^j$ vanish on each element of $\mathcal{T}_j$ for $cG(1)dG(0)$ elements and could equivalenty be included if we understand $\bar{SD}_\delta^j$ as a sum of the contributions on the spacial elements. With this interpretation, the stabilization term vanishes for sufficiently regular solutions of the Navier-Stokes equations (e.g., (2.3) and $\tilde{\boldsymbol{v}} \in L^2(I, H^2(\Omega)^2), \tilde{p} \in L^2(I, H^1(\Omega))$).

The stabilization parameters $\tilde{\delta}_1$ and $\tilde{\delta}_2$ act as a subgrid model in the convection-dominated case by adding a viscosity roughly of the local mesh size, see [19].

In order to obtain gradients which are exact on the discrete level, we consider the discrete Lagrangian functional based on the $cG(1)dG(0)$ finite element method, which is given by

$$\begin{aligned}&\mathcal{L}^h((\boldsymbol{v}_h,p_h),\tau_h,(\boldsymbol{\lambda}_h,\mu_h)) = J^h((\boldsymbol{v}_h,p_h),\tau_h)\\ &+\underbrace{\sum_{j=1}^{N} k_j\left(E^{h,j}((\boldsymbol{v}_h,p_h),\tau_h),(\boldsymbol{\lambda}_h,\mu_h)\right)}_{=:(E^h((\boldsymbol{v}_h,p_h),\tau_h),(\boldsymbol{\lambda}_h,\mu_h))} + \underbrace{\sum_{j=1}^{N} k_j\left(SD_\delta^j((\boldsymbol{v}_h,p_h),\tau_h),(\boldsymbol{w}_h,q_h)\right)}_{=:(SD_\delta((\boldsymbol{v}_h,p_h),\tau_h),(\boldsymbol{w}_h,q_h))}.\end{aligned}$$

To obtain the discrete adjoint equation and the reduced gradient, we take the derivatives of the discrete Lagrangian w.r.t. the state variables and the shape variables, respectively. Similar to the discrete state equation, the discrete adjoint system can be cast in the form of an implicit time-stepping scheme, backward in time, see [6].

For the computation of shape derivatives on the discrete level we use a transformation space $T_h(\Omega_{\text{ref}})$ of piecewise linear continuous functions. Then a discrete version of Lemma 2.2 holds, and we get an analogue of (2.7) on the discrete level. Thus, we obtain the exact shape derivative on the discrete level by using a continuous adjoint approach without the tedious task of computing mesh sensitivities.

## 4. Goal-oriented error estimation and adaptivity

In this section we investigate the use of goal-oriented a posteriori error estimation and adaptivity in the context of shape optimization. Goal-oriented error estimators based on duality arguments date back to a series of papers by Babuška and Miller, starting with [1], and were systematically investigated in the sequel, see, e.g., [11, 3]. They have already successfully been applied to optimal control and parameter identification problems, both for the elliptic and the parabolic case, see [2, 3, 23]. Goal-oriented estimators measure the error in a quantity of interest depending on the state, rather than the state itself. Thus, in the adaptive process, the computational domain is only resolved more accurately in areas which have an influence on the quantity of interest, which in our case is the objective function value.

### 4.1. Goal-oriented error estimation in shape optimization

In the context of shape optimization problems governed by the instationary Navier-Stokes equations, certain difficulties arise which keep us from directly using goal-oriented error estimators for optimal control problems as in, e.g., [2]. In particular, we use a nonconforming time discretization, i.e. $Y_h \not\subseteq Y$, which has also been considered in [23], and $T_h \not\subseteq T$. This means

that $\mathcal{L}'(y,\tau,\lambda)(\bar{y},\bar{\tau},\bar{\lambda}) = 0$ for $(\bar{y},\bar{\tau},\bar{\lambda}) \in Y_h \times T_h \times Z_h^*$ is not satisfied automatically. Furthermore, we introduce additional stabilization terms which contribute to the error estimator, and $E^h$ and $J^h$ contain additional jump terms compared to their continuous counterparts.

To overcome these difficulties, we assume for the continuous optimal solution $(y,\tau)$ that $E^h(y,\tau)' = E(y,\tau)'$, $J^h(y,\tau)' = J(y,\tau)'$, and $SD_\delta(y,\tau) = 0$ (i.e. the stabilization is consistent), and that

$$J'(y,\tau)(\bar{y}_h,\bar{\tau}_h) + \langle \lambda, E'(y,\tau)(\bar{y}_h,\bar{\tau}_h,\bar{\lambda}_h)\rangle = 0 \quad \forall (\bar{y}_h,\bar{\tau}_h,\bar{\lambda}_h) \in Y_h \times T_h \times Z_h^*.$$

We will see that these assumptions are satisfied for the considered $cG(1)dG(0)$ method if the continuous state and adjoint are sufficiently regular.

Assuming further that $J$ and $E$ are three times Gateaux-differentiable and $(y,\tau,\lambda) \in Y \times T \times Z^*$ and $(y_h,\tau_h,\lambda_h) \in Y_h \times T_h \times Z_h^*$ are stationary points of the continuous and discrete Lagrange functionals, resp., the a posteriori error with respect to the objective functional is given by

$$\begin{aligned} J(y,\tau) - J^h(y_h,\tau_h) = \frac{1}{2}\rho^y(y_h,\tau_h,\lambda_h)(\lambda - i_h\lambda) \\ + \frac{1}{2}\rho^\lambda(y_h,\tau_h,\lambda_h)(y - i_h y) + \frac{1}{2}\rho^\tau(y_h,\tau_h,\lambda_h)(\tau - i_h\tau) + \mathcal{R}, \end{aligned} \tag{4.1}$$

in terms of the residuals of the first order derivatives of the discrete Lagrangian (including the stabilization terms), where $i_h\lambda$, $i_h y$, and $i_h\tau$ are arbitrary approximations and the remainder $\mathcal{R}$ is of third order. Below we will state appropriate spaces for state and adjoint such that the required differentiability properties hold.

To arrive at a computable error estimator, we drop the residual $\mathcal{R}$. As the exact solution is unknown, we have to approximate the interpolation errors using linear operators: $\Pi_h y_h \approx (y - i_h y)$, $\Pi_h\lambda_h \approx (\lambda - i_h\lambda)$ and $\Pi_h\tau_h \approx (\tau - i_h\tau)$. Thus, we arrive at the computable error estimator

$$\begin{aligned} J(y,\tau) - J^h(y_h,\tau_h) \approx \frac{1}{2}\rho^\lambda(y_h,\tau_h,\lambda_h)(\Pi_h y_h) \\ + \frac{1}{2}\rho^y(y_h,\tau_h,\lambda_h)(\Pi_h\lambda_h) + \frac{1}{2}\rho^\tau(y_h,\tau_h,\lambda_h)(\Pi_h\tau_h). \end{aligned}$$

The interpolation errors are approximated by interpolating the discrete solution into higher order finite element spaces. In our computations, we interpolate the computed state and adjoint into the space of functions that are continuous, piecewise linear in time and discontinuous, piecewise quadratic on patches of elements in space.

### 4.2. Application to the Navier-Stokes equations

To apply the goal-oriented error estimator derived in the previous section to the instationary Navier-Stokes equations, we have to verify the assumptions made in section 4.1. We consider first the case of an inf-sup stable pair of finite elements in space for the state and adjoint. Then no stabilization is needed and we drop the terms $SD_\delta$ in the scheme. Under the assumptions of Lemma 2.1 the additional jump terms in $J^h$ and $E^h$ in comparison to $J$ and $E$ vanish. If the objective functional has a structure such that $\tilde{\mathbf{\lambda}}(T) \in H(\Omega)$

and that the right hand side of the adjoint equation is in $L^2(I;H^{-1}(\Omega)^2)$ then the adjoint state satisfies $\tilde{\boldsymbol{\lambda}} \in W(I;V(\Omega))$, see for example [17]. Then we can show that the assumptions of section 4.1 hold and that we obtain the error representation (4.1) with a remainder term of the form

$$\begin{aligned}\mathcal{R} = O\Big( &\big(\|\boldsymbol{v} - i_h\boldsymbol{v}\|_{L^2(I;H_0^1(\Omega_{\mathrm{ref}})^2)} + \|\boldsymbol{v}_t - (I^h(i_h\boldsymbol{v}))_t\|_{L^1(I;L^2(\Omega_{\mathrm{ref}})^2)} \\ &+ \|\boldsymbol{\lambda} - i_h\boldsymbol{\lambda}\|_{L^\infty(I;L^2(\Omega_{\mathrm{ref}})^2)} + \|\boldsymbol{\lambda} - i_h\boldsymbol{\lambda}\|_{L^2(I;H_0^1(\Omega_{\mathrm{ref}})^2)} \\ &+ \|p - i_h p\|_{L^2(I;L_0^2(\Omega_{\mathrm{ref}}))} + \|\mu - i_h\mu\|_{L^2(I;L_0^2(\Omega_{\mathrm{ref}}))} \\ &+ \|\tau - i_h\tau\|_{W^{1,\infty}(\Omega_{\mathrm{ref}})^2}\big)^3\Big),\end{aligned} \tag{4.2}$$

where $I^h(i_h\boldsymbol{v})$ denotes the continuous piecewise linear interpolation in time of $i_h\boldsymbol{v}$. Here, we assume that $J$ is three times continuously differentiable in the topology given by the norms in (4.2) (otherwise, the necessary norms would also appear). Other choices of the norms are possible. Furthermore, for a continuous, piecewise polynomial approximation of the transformations, $J'(y,\tau)(\bar{y}_h,\bar{\tau}_h)+\langle\lambda, E'(y,\tau)(\bar{y}_h,\bar{\tau}_h,\bar{\lambda}_h)\rangle = 0$ for all $(\bar{y}_h,\bar{\tau}_h,\bar{\lambda}_h) \in Y_h\times T_h\times Z_h^*$ is satisfied under our regularity assumptions on $\tilde{\boldsymbol{v}},\tilde{p},\tilde{\boldsymbol{\lambda}}$. For details we refer to [7].

In the presence of a streamline-diffusion type stabilization as considered in section 3, the continuous optimal solution has to be more regular in order to guarantee differentiability of the stabilization terms, for example $\tilde{\boldsymbol{v}},\tilde{\boldsymbol{\lambda}} \in L^2(I;H^2(\Omega)^2)$ and $\tilde{p},\tilde{\mu} \in L^2(I;H^1(\Omega))$. This is in particular the case if $\partial\Omega$ is of class $C^2$, the initial/end data are in $V(\Omega)$, and the source terms of state and adjoint equation are in $L^2(I;H(\Omega))$, see [30, Ch. III, Thm. 3.10] and [17]. The remainder term (4.2) contains then in particular the additional norms $\|\boldsymbol{v} - i_h\boldsymbol{v}\|_{L^\infty(I;H^1(\Omega_{\mathrm{ref}})^2)}$, $\|\nabla\boldsymbol{v} - \nabla i_h\boldsymbol{v}\|_{L^2(I;L^4(\Omega_{\mathrm{ref}})^2)}$, $\|\boldsymbol{\lambda} - i_h\boldsymbol{\lambda}\|_{L^\infty(I;H^1(\Omega_{\mathrm{ref}})^2)}$, $\|\nabla\boldsymbol{\lambda} - \nabla i_h\boldsymbol{\lambda}\|_{L^2(I;L^4(\Omega_{\mathrm{ref}})^2)}$, $\|p - i_h p\|_{L^2(I;H^1(\Omega_{\mathrm{ref}}))}$, $\|\mu - i_h\mu\|_{L^2(I;H^1(\Omega_{\mathrm{ref}}))}$. The proofs are lengthy and will be given in [7].

For example, the contribution of the momentum equation to the error estimator is given by

$$\begin{aligned}&\sum_{j=1}^{N}\int_{\Omega_{\mathrm{ref}}} ([\boldsymbol{v}_h]^{j-1})^T\ \Pi_h\boldsymbol{\lambda}_h^{j-1,+}\ \det\tau_h'\ dx \\ &\quad+\int_I\int_{\Omega_{\mathrm{ref}}}\sum_{i=1}^{d}\nu\nabla(v_{h,i})^T\tau_h'^{-1}\tau_h'^{-T}\ \nabla(\Pi_h\lambda_{h,i})\ \det\tau_h'\ dx\ dt \\ &\quad+\int_I\int_{\Omega_{\mathrm{ref}}}\boldsymbol{v}_h^T\tau_h'^{-T}\nabla\boldsymbol{v}_h\ \Pi_h\boldsymbol{\lambda}_h\det\tau_h'\ dx\ dt \\ &\quad-\int_I\int_{\Omega_{\mathrm{ref}}}p_h\ \mathrm{tr}(\tau_h'^{-T}\nabla(\Pi_h\boldsymbol{\lambda}_h))\det\tau_h'\ dx\ dt \\ &\quad-\int_I\int_{\Omega_{\mathrm{ref}}}\tilde{\boldsymbol{f}}(\tau_h(x),t)^T\ \Pi_h\boldsymbol{\lambda}_h\ \det\tau_h'\ dx\ dt,\end{aligned}$$

while the other terms are derived in the same fashion. Here, $[\boldsymbol{v}_h]^{j-1}$ denotes the jump of $\boldsymbol{v}_h$ at timestep $t_{j-1}$ and $\boldsymbol{\lambda}_h^{j-1,+}$ denotes the limit of $\boldsymbol{\lambda}_h$ for $t \searrow t_{j-1}$.

To drive the refinement process, we compute the local contributions to the global error on all pairs of spatial elements and time intervals. The local errors are computed by transforming the residual equations to the discrete physical domain and integrating cellwise by parts. For the momentum equation, the local error on element $K$ and time interval $I_j$ is thus approximated by

$$\left(R^{\tilde{\boldsymbol{v}}}(\tilde{y}_h), \widetilde{\Pi_h \boldsymbol{\lambda}_h}\right)_{I_j,K} + \left(r^{\tilde{\boldsymbol{v}}}(\tilde{y}_h), \widetilde{\Pi_h \boldsymbol{\lambda}_h}\right)_{I_j,\partial K} + \left([\tilde{\boldsymbol{v}}_h]^{j-1}, \widetilde{\Pi_h \boldsymbol{\lambda}_h}^{j-1,+}\right)_K,$$

with

$$R^{\tilde{\boldsymbol{v}}}(\tilde{y}_h)_{|K} := -\nu\Delta\tilde{\boldsymbol{v}}_h + \tilde{\boldsymbol{v}}_h^T\nabla\tilde{\boldsymbol{v}}_h + \nabla\tilde{p}_h - \tilde{\boldsymbol{f}}$$

$$r^{\tilde{\boldsymbol{v}}}(\tilde{y}_h)_{|e} := \begin{cases} \frac{1}{2}[\nu\partial_n\tilde{\boldsymbol{v}}_h - \tilde{p}_h\tilde{n}], & e \not\subset \partial\Omega \\ 0, & e \subset \partial\Omega \end{cases},$$

where $e$ denotes the edges of $K$.

*Remark* 4.1. Note that, in this section, we have neglected the presence of constraints on the admissible transformations $\tau$. For elliptic optimization problems, this has been investigated in [31].

## 5. Numerical results

We now demonstrate our results on numerical model problems. In the previous sections we considered homogeneous Dirichlet boundary conditions for the Navier-Stokes equations. In our numerical tests we will discuss problems with inflow, free outflow and noslip boundaries where we always impose a noslip condition on the boundary $\Gamma_B$ of the design object. However, we can also derive a formula for the reduced gradient in this setting as well as in the presence of the stabilization terms introduced by the $cG(1)dG(0)$ discretization.

When dealing with inflow and outflow boundaries, i.e. parts of the boundary where conditions of the form $\boldsymbol{v} = \boldsymbol{g} \in L^2(I; H^{1/2})$ and $\nu\partial_n\boldsymbol{v} - pn = 0$ hold, resp., we have to pay attention to some changes. For example in the presence of a free outflow boundary the correct space for the pressure is $L^2(\Omega)$ and not $L_0^2(\Omega)$. Since the admissible transformations equal the identity in a neighborhood of the inflow and outflow boundaries, there is no contribution to the shape derivative from these parts of the boundary. Moreover, for the adjoint equation, we obtain the boundary conditions $\boldsymbol{\lambda} = 0$ on the inflow boundary and, given sufficient regularity, $\nu\partial_n\boldsymbol{\lambda} + \boldsymbol{v}^T n\ \boldsymbol{\lambda} + \mu n = 0$ on the outflow boundary. Because a complete discussion of this setting is too long we will not go into further details. See also [5] and [29] for optimal control problems with the Navier-Stokes equations with inflow and outflow boundary conditions.

### 5.1. Shape Optimization with goal-oriented adaptivity

The first model problem is based on the DFG benchmark of a 2D instationary flow around a cylinder [27]. We prescribe a steady parabolic inflow profile on the left boundary with $v_{max} = 1.5m/s$, noslip boundary conditions on the top, bottom and object boundaries, and a free outflow condition on the right. The flow is modeled by the instationary incompressible Navier-Stokes equations with viscosity $\nu = 10^{-4}$, corresponding to a Reynolds number $Re \approx 400$ for the initial shape. Discretization is done using the $cG(1)dG(0)$ finite element method in Section 3. On the initial level of the adaptive refinement process, we start with a very coarse triangular spatial mesh with 2436 vertices and an initial uniform time step size $k = 10^{-3}$. For the adaptive mesh refinement we use a fixed-fraction strategy, refining 15% of the cells with the largest local errors with a red-green refinement algorithm; in addition, we refine 10% of the time intervals with the largest local error using bisection.

The object boundary $\Gamma_B$ is parameterized using a cubic B-Spline curve [25] with 7 control points for the upper half, which is reflected at the $y = 0.2$-axis to obtain a y-symmetric closed curve. This parameterization allows for apices at the front and rear of the object, while the remaining boundary is $C^2$. For the calculation of the reduced gradient we use a linear elasticity equation to extend the boundary displacement to the domain as described in section 2.6. We impose constraints on the volume of the object $B$ as well as bound constraints on the control points. The volume of $B$ can be evaluated analytically as a function of the B-spline control points by expressing the volume as a boundary integral.

We minimize the mean value of the drag on the object boundary $\Gamma_B$ over the time interval $[0, T]$, given by the formula

$$J((\tilde{\boldsymbol{v}}, \tilde{p}), \Omega) = \frac{1}{T} \int_0^T \int_\Omega \left( (\tilde{\boldsymbol{v}}_t + (\tilde{\boldsymbol{v}} \cdot \nabla)\tilde{\boldsymbol{v}} - \tilde{\boldsymbol{f}})^T \boldsymbol{\Phi} - \tilde{p} \operatorname{div} \boldsymbol{\Phi} + \nu \nabla \tilde{\boldsymbol{v}} : \nabla \boldsymbol{\Phi} \right) dx\, dt.$$

Here, $\boldsymbol{\Phi}$ is a smooth function such that with a unit vector $\boldsymbol{\phi}$ pointing in the mean flow direction holds $\quad \boldsymbol{\Phi}|_{\Gamma_B} \equiv \boldsymbol{\phi}, \quad \boldsymbol{\Phi}|_{\partial\Omega \setminus \Gamma_B} \equiv 0 \quad \forall \Omega \in \mathcal{O}_{\text{ad}}$.
This formula is an alternative formula for the mean value of the drag on $\Gamma_B$,

$$c_d := \frac{1}{T} \int_0^T \int_{\Gamma_B} \boldsymbol{n} \cdot \sigma(\tilde{\boldsymbol{v}}, \tilde{p}) \cdot \boldsymbol{\phi}\, dS,$$

with normal vector $n$ and stress tensor $\sigma(\tilde{\boldsymbol{v}}, \tilde{p}) = \nu(\nabla \tilde{\boldsymbol{v}} + (\nabla \tilde{\boldsymbol{v}})^T) - \tilde{p}\, I$, and can be obtained through integration by parts. For a detailed derivation, see [18].

Computation of the state, adjoint and shape derivative equations is done using Dolfin [21]. The optimization is carried out using a SQP solver written in Matlab, with a BFGS-approximation for the reduced Hessian.

Table 1 summarizes the computed results for the adaptive shape optimization problem. The columns contain from left the refinement level, the number of vertices, the number of timesteps $N$, the optimal objective function value $J$, the value of the (signed) global error $\eta$ and the number of SQP-iterations.

| level | vertices | N | J | $\eta$ | SQPit |
|---|---|---|---|---|---|
| 0 | 2436 | 2001 | 0.0330721648 | −0.00542514 | 12 |
| 1 | 4283 | 2200 | 0.0314016876 | −0.00273496 | 5 |
| 2 | 7875 | 2419 | 0.0325643722 | 0.000807385 | 4 |
| 3 | 13666 | 2658 | 0.0336900832 | 0.00145268 | 2 |
| 4 | 24396 | 2923 | 0.0339111094 | 0.00132779 | 2 |

Table 1: Optimization Results

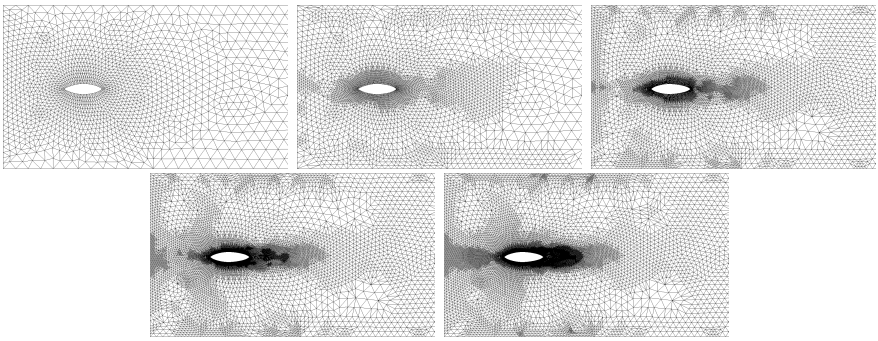

Figure 1: Comparison of the meshes for the optimal shape on different refinement levels

On the higher refinement levels, the differences between the objective function values decrease. Most importantly, the number of SQP iterations reduces on the higher levels. Thus, most of the optimization iterations are performed on the cheap coarser grids, significantly reducing the amount of computational work. Furthermore, we obtain meshes that are well adapted to the evaluation of the drag objective function value. Figure 1 shows the computational meshes for the optimal shape on the refinement levels. The adaptive refinement primarily takes place in the vicinity of the object and in its wake. The instationary, time-periodic behavior of the flow starts to be resolved on level 2 and is only fully resolved on levels 3 and 4, which explains the increase in the error estimator from level 2 to 3.

### 5.2. Shape optimization with two objects

The shape derivative calculus that was introduced in section 2 can readily be applied to shape optimization problems with more than one object.

Figure 2 shows the optimal solution for a shape optimization problem with two objects in a row, where the drag was minimized for a flow governed by the stationary Navier-Stokes equations with $\nu = 10^{-2}$. The design parameters are the grid points on the boundary curve with 80 boundary points per object and separate volume constraints are imposed on both objects. The

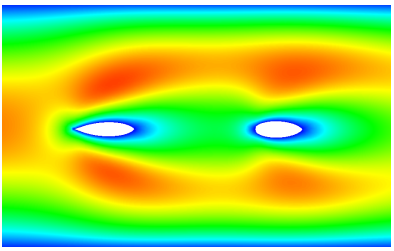

Figure 2: Flow around 2 objects

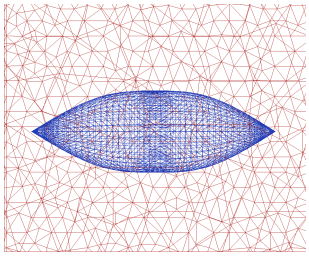

Figure 3: 3D object

front point of the first object is fixed while the front point of the second object can move in x-direction within box constraints. In the optimal solution the second object took the maximum distance to the first object. The optimization was carried out using Ipopt [32], while the computation of the state, adjoint and shape derivative equations was done with Sundance [22].

### 5.3. Shape optimization in three dimensions

Currently we are extending our approach to three dimensional problems. While transferring the equations is straightforward, solving the arising systems of equations becomes numerically challenging due to the huge amount of degrees of freedom. Therefore, techniques such as multigrid methods and problem specific preconditioners, in conjunction with adaptive mesh refinement, have to be used.

Solving the state equation includes the successive solve of linear systems of the form $\left(\begin{smallmatrix} F & \tilde{B}^T \\ B & C \end{smallmatrix}\right)\left(\begin{smallmatrix} s_v \\ s_p \end{smallmatrix}\right) = b$. We analyzed different solvers and preconditioners in this context and finally use GMRESR with the SIMPLEC preconditioner [10]. The preconditioner needs to solve two subsystems for $F^{-1}$ and for the approximation of the Schur complement. Numerical tests showed that we need to solve these subsystems only up to precision $10^{-3}$ which is done by BiCGStab with an algebraic multigrid preconditioner. The implementation is done in Trilinos [16] and uses parallelization on 16 processors.

Figure 3 shows the optimal shape for a 3D object which is parameterized with cubic B-spline surface patches. The mean value of the drag was minimized for a flow governed by the instationary Navier-Stokes equations with $\nu = 10^{-4}$ under a volume constraint.

## 6. Conclusions

We have presented a continuous approach to shape optimization which is based on the instationary Navier-Stokes equations. In this setting the appropriate function spaces for the transformations and states were characterized and a differentiability result for the design-to-state operator was presented. The approach for calculating the shape gradients allows the solution of the

state and adjoint equation on the physical domain, hence existing solvers can be used. Furthermore, the approach is flexible enough to conveniently use arbitrary types of shape parameterizations, for example free form deformation or parameterized boundary displacements, also with multiple objects.

The combination with error estimators and multilevel techniques can reduce the number of optimization iterations on the fine grids and the necessary degrees of freedom significantly. Currently, the developed techniques are extended to 3-dimensional shape optimization problems.

## References

[1] I. Babuška and A. Miller, *The post-processing approach in the finite element method. Part 1: Calculation of displacements, stresses and other higher derivatives of the displacements*, Int. J. Numer. Methods Eng., 20, pp. 1085–1109, 1984.

[2] R. Becker and H. Kapp and R. Rannacher, *Adaptive finite element methods for optimal control of partial differential equations: Basic concepts*, SIAM J. Control Optim., 39(1), pp. 113–132, 2000

[3] R. Becker and R. Rannacher, *An optimal control approach to a posteriori error estimation in finite element methods*, Acta Numerica 10, pp. 1–102, 2001

[4] J. A. Bello, E. Fernandez-Cara, J. Lemoine, and J. Simon, *The differentiability of the drag with respect to the variations of a Lipschitz domain in Navier-Stokes flow*, SIAM J. Control Optim., 35(2), pp. 626–640, 1997

[5] M. Berggren, *Numerical solution of a flow-control problem: vorticity reduction by dynamic boundary action*, SIAM J. Sci. Comput. 19, no. 3, pp. 829–860, 1998

[6] C. Brandenburg, F. Lindemann, M. Ulbrich, and S. Ulbrich, *A continuous adjoint approach to shape optimization for Navier Stokes flow*, in *Optimal control of coupled systems of partial differential equations*, K. Kunisch, G. Leugering, and J. Sprekels, Eds., Int. Ser. Numer. Math. 158, Birkhäuser, Basel, pp. 35–56, 2009

[7] C. Brandenburg and S. Ulbrich, *Goal-oriented error estimation for shape optimization with the instationary Navier-Stokes equations*, Preprint in preparation, Fachbereich Mathematik, TU Darmstadt, 2010.

[8] K. K. Choi and N.-H. Kim, *Structural sensitivity analysis and optimization 2: Nonlinear systems and applications*, Mechanical Engineering Series, Springer, 2005

[9] M. C. Delfour and J.-P. Zolésio, *Shapes and geometries: Analysis, differential calculus, and optimization*, SIAM series on Advances in Design and Control, 2001

[10] J. Doormaal and G.D.Raithby, *Enhancements of the SIMPLE method for predicting incompressible fluid flows*, Num. Heat Transfer, 7, pp. 147–163, 1984

[11] K. Eriksson, D. Estep, P. Hansbo, and C. Johnson, *Introduction to adaptive methods for differential equations*, Acta Numerica, pp 105–158, 1995

[12] K. Eriksson, D. Estep, P. Hansbo, and C. Johnson, *Computational differential equations*, Cambridge University Press, 1996

[13] M. Geissert, H. Heck, and M. Hieber, *On the equation* $\operatorname{div} u = g$ *and Bogovski's operator in Sobolev spaces of negative order*, in *Partial differential equations and functional analysis*, E. Koelink, J. van Neerven, B. de Pagter, and G. Sweers, Eds., Oper. Theory Adv. Appl., 168, Birkhäuser, Basel, pp. 113–121, 2006.

[14] P. Guillaume and M. Masmoudi, *Computation of high order derivatives in optimal shape design*, Numer. Math., 67, pp. 231–250, 1994

[15] J. Haslinger and R. A. E. Mäkinen, *Introduction to shape optimization: Theory, approximation, and computation*, SIAM series on Advances in Design and Control, 2003

[16] M. A. Heroux, J. M. Willenbring, and R. Heaphy, *Trilinos developers guide*, Sandia National Laboratories, SAND2003-1898, 2003

[17] M. Hinze, *Optimal and instantaneous control of the instationary Navier-Stokes equations*, Habilitation, TU Dresden, 2002.

[18] J. Hoffman and C. Johnson, *Adaptive Finite Element Methods for Incompressible Fluid Flow*, Error estimation and solution adaptive discretization in CFD: Lecture Notes in Computational Science and Engineering, Springer Verlag, 2002.

[19] J. Hoffman and C. Johnson, *A new approach to computational turbulence modeling*, Comput. Meth. Appl. Mech. Engrg., 195, pp. 2865–2880, 2006

[20] F. Lindemann, M. Ulbrich, and S. Ulbrich, *Fréchet differentiability of time-dependent incompressible Navier-Stokes flow with respect to domain variations*, Preprint in preparation, Fakultät für Mathematik, TU München, 2010.

[21] A. Logg and G. N. Wells, *DOLFIN: Automated finite element computing*, ACM Transactions on Mathematical Software, 37(2), 2010

[22] K. Long, *Sundance: A rapid prototyping tool for parallel PDE-constrained optimization*, in *Large-scale pde-constrained optimization*, L. T. Biegler, M. Heinkenschloss, O. Ghattas, and B. van Bloemen Wanders, Eds., Lecture Notes in Computational Science and Engineering, 30, Springer, pp. 331–341, 2003

[23] D. Meidner and B. Vexler, *Adaptive space-time finite element methods for parabolic optimization problems*, SIAM J. Control Optim., 46, pp 116–142, 2007

[24] B. Mohammadi and O. Pironneau, *Applied shape optimization for fluids*, Oxford University Press, 2001

[25] M. E. Mortensen, *Geometric modeling*, Wiley, 1985

[26] F. Murat and S. Simon, *Etudes de problems d'optimal design*, Lectures Notes in Computer Science, 41, pp. 54–62, 1976

[27] M. Schäfer and S. Turek, *Benchmark computations of laminar flow around a cylinder*, Preprints SFB 359, No. 96-03, Universität Heidelberg, 1996

[28] J. Sokolowski and J.-P. Zolésio, *Introduction to shape optimization*, Series in Computational Mathematics, Springer, 1992

[29] T. Slawig, *PDE-constrained control using Femlab – Control of the Navier-Stokes equations*, Numerical Algorithms, 42, pp. 107–126, 2006

[30] R. Temam, *Navier-Stokes equations: Theory and numerical analysis* 3rd Edition, Elsevier Science Publishers, 1984

[31] B. Vexler and W. Wollner, *Adaptive finite elements for elliptic optimization problems with control constraints*, SIAM J. Control Optim., 47, pp 509–534, 2008

[32] A. Wächter and L. T. Biegler, *On the implementation of a primal-dual interior point filter line search algorithm for large-scale nonlinear programming*, Math. Program., 106, pp. 25–57, 2006

Christian Brandenburg
Fachbereich Mathematik
Technische Universität Darmstadt
Dolivostr. 15
64293 Darmstadt
Germany
e-mail: brandenburg@mathematik.tu-darmstadt.de

Florian Lindemann
Lehrstuhl für Mathematische Optimierung
Zentrum Mathematik, M1
TU München
Boltzmannstr. 3
85747 Garching bei München
e-mail: lindemann@ma.tum.de

Michael Ulbrich
Lehrstuhl für Mathematische Optimierung
Zentrum Mathematik, M1
TU München
Boltzmannstr. 3
85747 Garching bei München
e-mail: mulbrich@ma.tum.de

Stefan Ulbrich
Fachbereich Mathematik
Technische Universität Darmstadt
Dolivostr. 15
64293 Darmstadt
Germany
e-mail: ulbrich@mathematik.tu-darmstadt.de